



Removal of Cr(VI) from wastewater using activated neem bark in a fixed-bed column: interference of other ions and kinetic modelling studies

Utkarsh Maheshwari, Suresh Gupta*

Department of Chemical Engineering, Birla Institute of Technology and Science (BITS), Pilani 333031, Rajasthan, India, emails: utkarsh@pilani.bits-pilani.ac.in, utkarshmaheshwari13@gmail.com (U. Maheshwari), Tel. +91 1596 515224; Fax: +91 1596 244183; email: sureshg@pilani.bits-pilani.ac.in (S. Gupta)

Received 6 October 2014; Accepted 9 February 2015

ABSTRACT

Continuous adsorption experiments are carried out in a fixed-bed to evaluate the performance of a newly developed low-cost adsorbent (activated neem bark, ANB) for the removal of Cr(VI) along with other metal ions (Cu & Zn) from aqueous solutions. The effect of initial Cr(VI) concentration, mass of adsorbent and flow rate on the breakthrough curve are studied. It is observed that as there is an increase in the initial concentration of Cr(VI) from 50 to 100 mg L⁻¹, the mass of the adsorbent from 25 to 175 g, and flow rate from 5 to 15 mg L⁻¹, the breakthrough time decreases from 24.78 to 13.875 h, increase from 9.25 to 111.66 h and decrease from 35.09 to 8.26 h, respectively. The effect on the performance of the ANB for Cr(VI) adsorption is also studied in the presence of Cu and Zn. The breakthrough time is achieved earlier in the presence of Cu and Zn in the feed stream. The fixed-bed adsorption process parameters such as saturation loading capacity, breakthrough time, total percentage removal of Cr(VI), the fraction of unused bed length, adsorption exhaustion rate and empty bed residence time are calculated for different experimental runs. The experimental results are likewise applied to the Yoon–Nelson and the Yan kinetic models. The kinetic parameters for both the models are calculated and reported in this study.

Keywords: Adsorption; Multiple metal ions; Continuous studies; Breakthrough curve parameters; Yoon & Nelson model; Yan model

1. Introduction

With the modernization and industrialization, there are a huge number of pollutants present in the atmosphere. Heavy metals are one of the toxic pollutants present in the atmosphere. These are segregated from other toxic pollutants due to their non-biodegradable nature and their consequence on the living beings. The heavy metals can accumulate in the body through the food chain. Even the presence of a small amount of the

heavy metals can lead to a severe physiological and neurological damage to the living beings [1]. Throughout the world, there is a vast presence of hexavalent chromium ion (Cr(VI)) in the industrial effluent streams as weighing against any other metal contaminants. The compounds of Cr(VI) are utilized in various industries such as fungicides, glass, tanning, ceramics, rubber, metallurgical, fertilizers, mining, textile, paper and pulp. The effluent from these industries contains a very high amount of Cr(VI) along with other metal ions (Cu, Zn, Co, Zn, Mg, Ni, Pb, etc.) and causing a

*Corresponding author.

brutal environmental and public health problems. Cr(VI) is a highly mobile metal and according to the World Health Organization, the permissible limit of Cr(VI) in wastewater is 0.1 mg L^{-1} beyond which it is considered acutely toxic, carcinogenic and mutagenic to the living organisms, and hence more unsafe than other heavy metals [1,2].

To keep the metal contamination in the effluent of these industries up to a permissible limit, there is a dire need for the treatment of effluent streams before sending it to the outer water bodies such as river, lake and pond. There are a number of methods available in the literature for the removal of Cr(VI) from industrial wastewater, such as ion exchange, electrochemical precipitation, solvent extraction, adsorption and reverse osmosis [3–7]. However, most of the industrial effluents contain multiple metal ions and adsorption is one among all the separation processes, capable of simultaneously removing multiple heavy metals from the industry effluents in an efficient and cost-effective manner. The adsorption process becomes more economical, when the low-cost adsorbent can be keyed out and utilized for the operation [8,9].

In most of the reported studies, the utilization of the low-cost adsorbents is limited to the batch mode [9–14]. Very few studies have reported the continuous mode of operation for the removal of single metal ions from wastewater [15–21]. The removal of multiple metal ions from wastewater using continuous mode of adsorption process is not much explored.

A fixed-bed column, packed with suitable adsorbent, is the most efficient arrangement for the removal of heavy metals. The design of an adsorption column depends on a range of key parameters such as flow rate, inlet metal concentration and bed height, that is mass of adsorbent. To have a better understanding of the adsorption process, the determination of the break point time of the operation and per cent utilization of the bed up to the break point is necessary. These values would be helpful in estimating the performance of adsorption column and in the designing of large-scale operations [8].

In this study, activated neem bark (ANB) is prepared as low-cost adsorbents and is utilized for the removal of Cr(VI) from wastewater by conducting continuous experiments. Continuous adsorption experiments are carried out to establish the effect of process parameters such as bed height (mass of adsorbent), flow rate and the initial Cr(VI) concentration on Cr(VI) removal. The effect of the presence of multiple metal ions (Cu & Zn) along with Cr(VI) on the break-through time is also studied. The Yoon–Nelson and Yan model are applied to the experimental data to estimate the various kinetic parameters.

2. Materials and methods

2.1. Adsorbent preparation

Neem bark is obtained from the neem trees of Birla Institute of Technology and Science, Pilani, Rajasthan, India. It is repetitively rinsed with distilled water for the removal of dust and soluble impurities present on it. It is further kept for drying in the shade at room temperature for 24 h. The dried bark is crushed into little parts in a series of crushing and mashing with the aid of roller crusher, jaw crusher and ball mill. The crushed neem bark pieces are passed through 12–14 BSS mesh screens. The neem bark pieces retained on the 14 mesh screen, with a particle size (d_p) of approximately 1.20 mm, are used as an adsorbent for the experiments.

The obtained neem bark is activated by a proper chemical and physical activation process. The neem bark is treated with concentrated H_2SO_4 (98%) on 1:1 weight basis and then kept it in the oven in a closed glass container at 70°C for 24 h. Later, the ANB is repeatedly washed in distilled water to remove colour impurities and traces of acids present in it.

2.2. Characterization

The developed ANB is being characterized using various characterization techniques. The morphology of the developed adsorbent is studied using scanning electron microscope (SEM). Energy dispersive spectroscopy (EDS) is used to detect the elements present in the developed adsorbent and their composition in terms of the weight fraction. The SEM and EDS of the developed adsorbent are performed using field emission gun-scanning electron microscope (JSM-7600F). X-ray diffraction (XRD) is useful to examine the form of the developed adsorbent and is performed using Rigaku Mini Flex II Desktop X-ray model. The surface area of the developed adsorbent is determined using the Brunauer–Emmett–Teller surface area analyser (Smart Sorb 92/93, Smart Instruments Co. Pvt. Ltd.). The Fourier transform infra red (FTIR) spectroscopy is done for the developed ANB using Frontier model, Perkin Elmer, which provides the absorption peaks according to the various chemical groups present in the adsorbent surface. Thermogravimetric analysis (TGA) is also performed on the developed ANB using a Thermogravimetric analyzer (TGA - 4000, Perkin Elmer). This would help in understanding the thermal stability of the adsorbent.

2.3. Experimental studies

2.8287 g of 99.9% potassium dichromate ($\text{K}_2\text{Cr}_2\text{O}_7$) is dissolved in distilled water, and volume of the

solution is made up to 1,000 ml to prepare a 1,000 mg L⁻¹ stock solution of Cr(VI). The stock solution is diluted as required to obtain standard solutions containing 50–100 mg L⁻¹ of Cr(VI).

Continuous experiments are performed for the removal of Cr(VI) from aqueous solutions using ANB as a packing material in a fixed-bed column. The schematic diagram of the experimental set-up is shown in Fig. 1. A glass column of 2.53 cm inner diameter is employed as a fixed-bed column. The column is packed with the ANB in a stepwise manner. Primarily, a known quantity of ANB is filled into the column and is shaken manually in order to have intense packing. The pattern is extended till the total amount of the adsorbent is packed into the column. Later, 500 ml of distilled water is passed through the bed to ensure an added dense packing. The prepared aqueous solution of Cr(VI) is passed through the fixed-bed column in the down flow mode. A constant flow rate is maintained using the liquid rotameter (5–15 ml min⁻¹). In the present work, the parameters varied are the mass of adsorbent, the inlet flow rate and the inlet Cr(VI) concentration. An optimum pH value (=2) obtained from the batch experiments is maintained throughout the continuous experiments [22]. The other criteria for considering this pH value is the low pH value of the

actual industrial effluents. The various industrial effluents such as chromium plating effluent (pH 1) [23], tannery effluent (pH 2) [24] and electro-plating effluent (pH 2.2) [25], and the reported experimental studies in the literature [26] are having low pH value. The performance of the ANB for the synthetically prepared multiple ions industrial solution (50 mg L⁻¹ each of Cr, Cu and Zn) is also analysed.

In this study, Atomic Absorption Spectrophotometer (AA-7000, Shimadzu) is used to determine the amount of total Cr, Cu and Zn ions in the aqueous solutions. All the experiments are repeated twice to ensure the repeatability.

2.4. Modelling of continuous adsorption process

The design of fixed-bed adsorption column is very complicated. If the mathematical model is developed and proposed based on the proper understanding of the adsorption system, then it would be helpful in proposing the suitable design of the large-scale adsorption column. The behaviour of the adsorption column can be well understood by the plot of outlet adsorbate concentration vs. time, which is seldom termed as the breakthrough curve. Breakthrough time and the shape of the curve are the important parameters for explaining the behaviour of adsorption column. Breakthrough time corresponds to the time required to reach the outlet concentration of pollutant to its permitted limit. In most of the cases, the breakthrough concentration is in the range of 1–5% of the feed concentration. Generally, the key factors affecting the breakthrough time are the column capacity or the column height, the flow rate and the feed concentration. As the time progress, the effluent concentration is increases from zero/low metal concentration to the inlet concentration. These results would be helpful in estimating the column capacity [27–29]. The continuous adsorption experiments are to be conducted in a fixed-bed column for obtaining the experimental data.

The total amount (stoichiometric) of Cr(VI) adsorbed (q_t , mg) in the column for given initial Cr(VI) concentration and flow rate is obtained using Eq. (1).

$$q_t = \frac{QA_c}{1,000} = \frac{Q}{1,000} \int_{t=0}^{t=t_{\text{total}}} C_{\text{ad}} dt \quad (1)$$

The quantity of A_c , that is the area underneath the curve, is acquired by plotting a graph of the adsorbed concentration (C_{ad} , mg L⁻¹) with respect to the time (t , min). Q is the flow rate during the process in

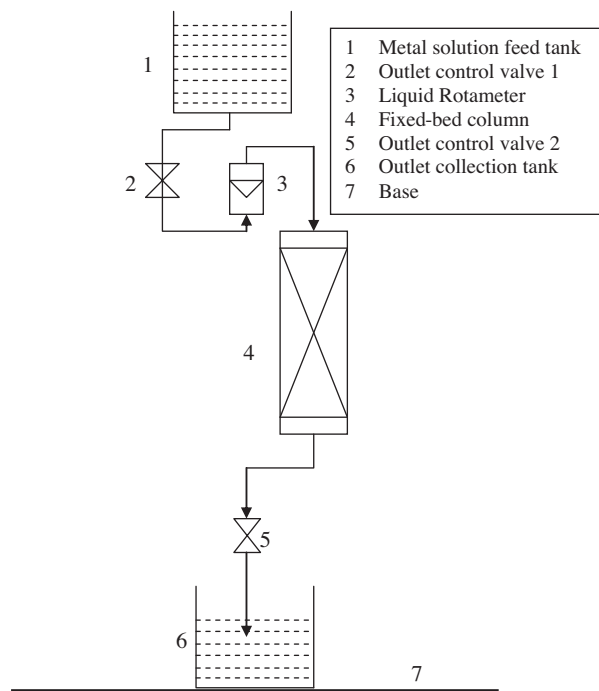


Fig. 1. Fixed-bed continuous adsorption experimental set-up for Cr(VI) removal from effluent.

ml min⁻¹. The amount of the total Cr(VI) passed through the column (m_t) can be evaluated using Eq. (2).

$$m_t = \frac{C_{bo}Q t_t}{1,000} \quad (2)$$

where t_t is the time equivalent to the total stoichiometric capacity of the fixed-bed column and is given by Eq. (3).

$$t_t = \frac{q_t t_f}{m_t} \quad (3)$$

where q_t is the amount of Cr(VI) adsorbed in time t and t_f is the total time of the process.

The amount of total Cr(VI) removed in terms of percentage is calculated using Eq. (4).

$$\text{Total percentage removal of Cr(VI) (S)} = \frac{q_t}{m_t} \times 100 \quad (4)$$

The empty bed residence time (EBRT), the total time needed to occupy the empty column is determined using Eq. (5).

$$\text{EBRT} = \frac{\text{Bed volume}}{\text{Volumetric flow rate of liquid}} \quad (5)$$

An additional parameter determined in the continuous experiments is the adsorbent exhaustion rate (R_a) which indicates the amount of the adsorbent (W) utilized on the basis of a unit volume of liquid treated till the breakthrough time. It can be obtained using Eq. (6).

$$\text{Adsorbent exhaustion rate (R}_a\text{)} = \frac{\text{Mass of adsorbent in column}}{\text{Volume treated at breakthrough}} \quad (6)$$

The fraction of the unused bed length (y) is evaluated using Eq. (7).

$$y = 1 - \frac{t_b}{t_t} \quad (7)$$

where t_b is the breakthrough time of the process.

Due to the complexity involved in understanding the behaviour of continuous adsorption process, Yoon–Nelson and Yan mathematical models are utilized for predicting the dynamic behaviour of the column [27,29,30].

2.4.1. The Yoon–Nelson model

A simple model is developed by Yoon–Nelson [31] which addresses the adsorption and the breakthrough process of the vapours or gases on the activated carbon. The model assumes that the rate of decrease in the probability of adsorption for each adsorbate molecule is proportional to the probability of sorbate sorption and the probability of a sorbate breakthrough on adsorbent [32]. The Yoon–Nelson equation with respect to a single component system is expressed using Eq. (8).

$$\frac{C_i}{C_{0,i}} = \frac{\exp(K_{YN,i} \times t - K_{YN,i} \times \tau_i)}{1 + \exp(K_{YN,i} \times t - K_{YN,i} \times \tau_i)} \quad (8)$$

where $K_{YN,i}$ represents the Yoon–Nelson rate constant of i^{th} component (h^{-1}), τ_i represents the time required for 50% of i^{th} adsorbate breakthrough (h), and t is the time (h) at which the samples are collected. The analysis of the breakthrough curves with the help of the model requires the evaluation of the model parameters $K_{YN,i}$ and τ_i .

2.4.2. The Yan model

The basis of the Yan model is the statistical analysis of the experimental results along with some of the simplifications [33]. Yan model is more trustworthy than other models because it explains the entire breakthrough curve with more precision. The model can be represented by Eq. (9).

$$\frac{C_i}{C_{0,i}} = 1 - \frac{1}{1 + \left(\left(\frac{0.001 \times C_{0,i} \times Q}{q_{0,i} \times M} \right) \times t \right)^{a_i}} \quad (9)$$

where a_i and $q_{0,i}$ are the Yan model parameters. Here, the relation between the model parameters with the experimental condition is impossible which leads to an impossible scaling up of the process [29].

3. Characterization

In this study, the surface morphology of the prepared adsorbent is being examined using SEM-EDS technique. The work is done at a magnification of 50,000X. The SEM and EDS analysis of fresh adsorbent and used adsorbent are shown in Figs. 2 and 3, respectively.

The images of SEM given in Figs. 2(a) and 3(a) provide the morphology of the developed adsorbent. These images also help in identifying the pore sizes

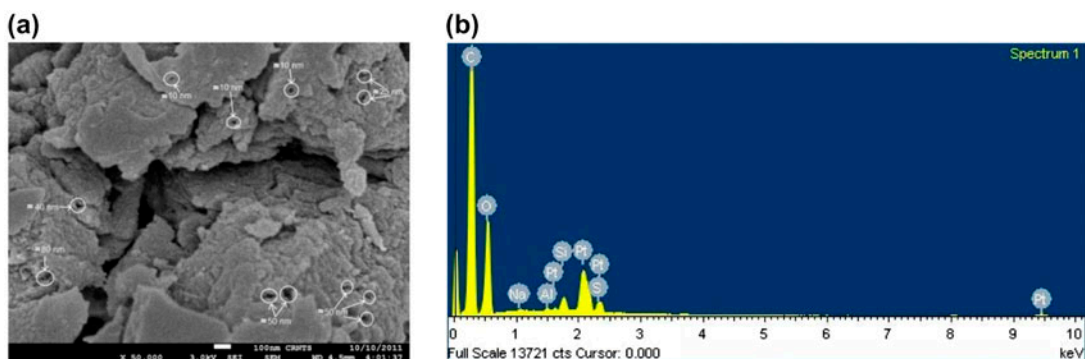


Fig. 2. (a) SEM and (b) EDS for fresh ANB.

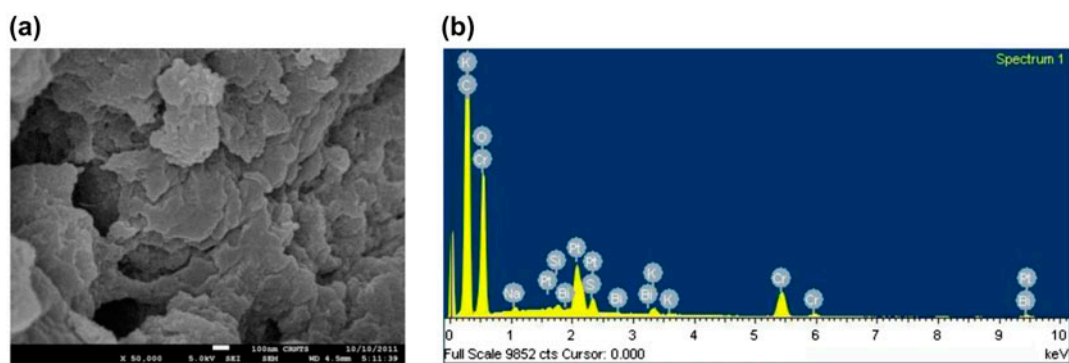


Fig. 3. (a) SEM and (b) EDS for used ANB on pure Cr(VI) solution.

available on the surface of the adsorbent which is an important characteristic of any developed adsorbent. The various markings shown in Fig. 2(a) are clearly indicated the availability of the smaller size pores on the surface of the developed adsorbent. The comparison of the pores while scaling the figure confirms the availability of nano size (10–100 nm) pores on the surface of the developed adsorbent. The EDS analysis given in Fig. 2(b) shows the elements available at the surface of the adsorbent, and it also provides their corresponding weight fractions. The utmost peak is for the carbon (C) which is roughly 55.35% of the overall adsorbent by weight. This may be due to the use of a carbonaceous material (neem bark) to develop the adsorbent. Also it confirms the unavailability of Cr(VI) in the fresh ANB.

The EDS analysis (Fig. 3(b)) confirms the presence of Cr(VI) in the saturated adsorbent which is approximately 10% by weight. It also shows the presence of 1.5% Potassium (K) by weight, which may be due to the utilization of potassium dichromate ($K_2Cr_2O_7$) for the preparation of the aqueous solution of the Cr(VI). Further analysis of SEM images (Figs. 2(a) and 3(a))

indicates that the pores available in the fresh ANB are not much visible in the saturated ANB. This confirms that the pores available for the adsorption are now occupied by the Cr(VI) molecules.

Fig. 4 represents the EDS analysis of ANB saturated with Cr(VI), Cu(II) and Zn(II). The presence of all the three metal ions is clearly visible on the adsorption sites. This analysis shows the presence of approximately 7% of Cr(VI), 2% of Zn(II) and 1% of Cu(II) by weight in the used adsorbent.

In this study, the surface area of the developed ANB is found to be about $36.64 \text{ m}^2 \text{ g}^{-1}$ which is higher as compared to various low-cost adsorbents such as tamarind seeds [34], tea factory waste [26], *Aspergillus niger* [35], Zn(O) particles [36] and sawdust [8]. The higher surface area is responsible for the availability of the more adsorption sites for the adsorption which leads to increase in the adsorption capacity [37,38].

The FTIR spectrum of the developed ANB is shown in Fig. 5. A wavy spectrum is obtained in place of a smooth one which confirms the amorphous nature of the developed ANB. According to the peaks identified at 670 & 2,900, 1,120, 1,540, 1,620 and

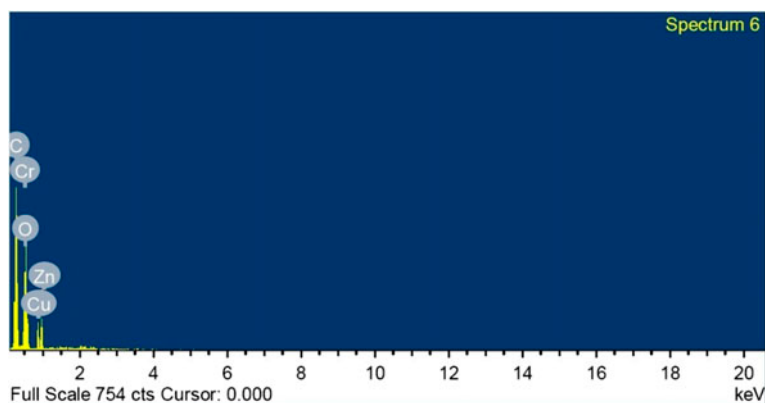


Fig. 4. EDS image for the saturated ANB utilized on the multiple metal ions.

$2,152\text{ cm}^{-1}$, confirms the presence of C–H, C–O, C=O, C=C and C≡C stretching vibrations, respectively. The availability of water molecules (i.e. O–H stretching mode of hydroxyl groups) is supported by the presence of a peak at $3,330\text{ cm}^{-1}$ [39,40]. The availability of various bonds of C–O and C=O suggests the availability of the various acidic groups on the surface of ANB [40,41]. After comparing the FTIR of the used and the fresh ANB, it is found that the peaks at $1,120$ and $3,330\text{ cm}^{-1}$ are reduced which indicate the utilization of C=O and O–H bonds during the adsorption process. The other peaks are approximately same in both the spectrums.

In the XRD analysis of ANB, Cu-K α radiation is employed by the diffractometer. 1.54 \AA is the wavelength considered for the analysis, and angle 2θ is varied in a range of $10\text{--}90^\circ$ with a step size of 0.01° . The XRD pattern for the ANB is shown in Fig. 6. The XRD pattern does not show any sharp peak. However, a broad peak can be observed which confirms the amorphous nature of the developed adsorbent. This is also

being confirmed by IR spectrum (Fig. 4) [42]. The particle size of developed adsorbent cannot be estimated using the Scherrer's formula due to the unavailability of the sharp peak [43].

TGA analysis of the developed ANB is shown in Fig. 7. It can be seen that there is a slow decrease up to 90 weight percentage and further to 82 when the temperature rises up to 100 and then reached to 240°C . The initial dip in the weight per cent may be due to the removal of surface moisture. Further increase in the temperature ($>240^\circ\text{C}$) results in the slow rate of pyrolysis and burning of the adsorbent. Finally, ANB completely converts into ash, when the temperature has reached approximately 550°C . Further increase in temperature will not affect the weight of ANB as there will be only ash left in the analysis chamber.

The result of TGA analysis indicates that the developed adsorbent is thermally stable up to 200°C . It can also be inferred that the saturated adsorbent could be regenerated at higher temperatures without any degradation of adsorbent.

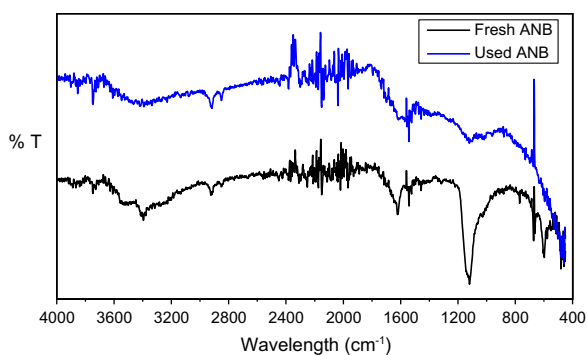


Fig. 5. FTIR spectra of fresh and used ANB from $4,000$ to 450 cm^{-1} wavelength.

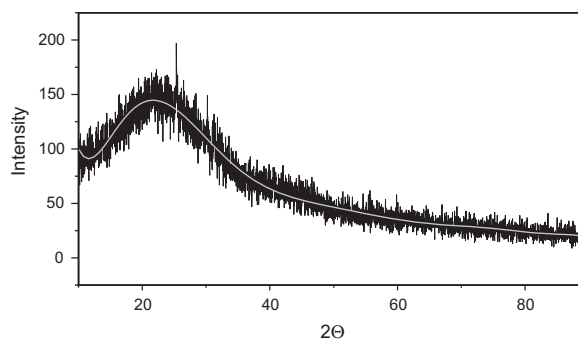


Fig. 6. Powder XRD pattern for ANB.

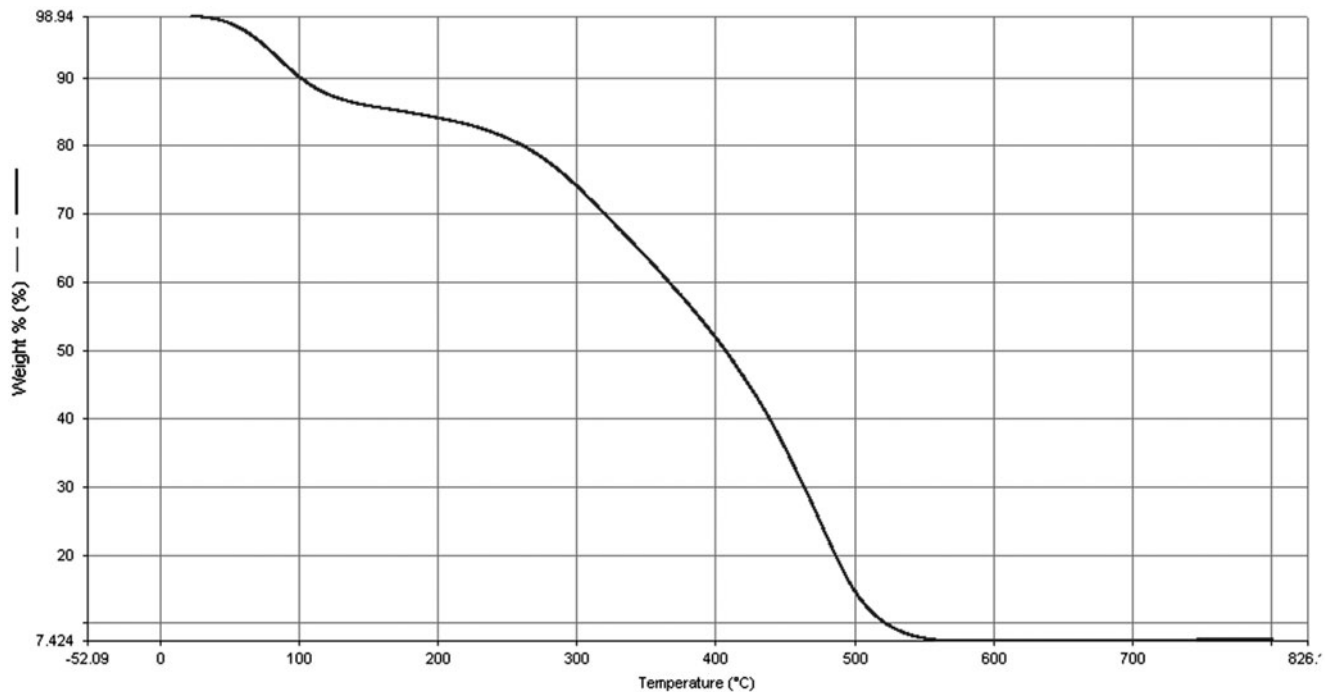


Fig. 7. TGA analysis of ANB.

4. Results and discussion

The equilibrium study of fresh neem bark and the ANB for the removal of Cr(VI) is already being conducted. The adsorption capacity of ANB was found to be approximately double to the capacity obtained for the removal of Cr(VI) using fresh neem bark [22,44]. In the succeeding sections, the consequence of various parameters such as the mass of adsorbent, the inlet flow rate, the inlet Cr(VI) concentration and interference of other ions on the continuous removal of Cr(VI) in a fixed-bed adsorption column is discussed.

4.1. Effect of initial inlet Cr(VI) concentration

The effect of the initial concentrations (50 and 100 mg L⁻¹) on the breakthrough curve for Cr(VI) adsorption from aqueous solution is shown in Fig. 8.

The various parameters such as the time corresponding to the breakthrough point (t_b), the time required to attain the total capacity of the column (t_t), the total flow time (t_f), the stoichiometric amount of Cr(VI) adsorbed (q_t), the quantity of Cr(VI) supplied to the column (m_t), the total percentage removal of Cr(VI) (S), the exhaustion rate of adsorbent (R_a), the EBRT and the fraction of the unused bed length (y) are calculated for each experimental run and are reported in Table 1.

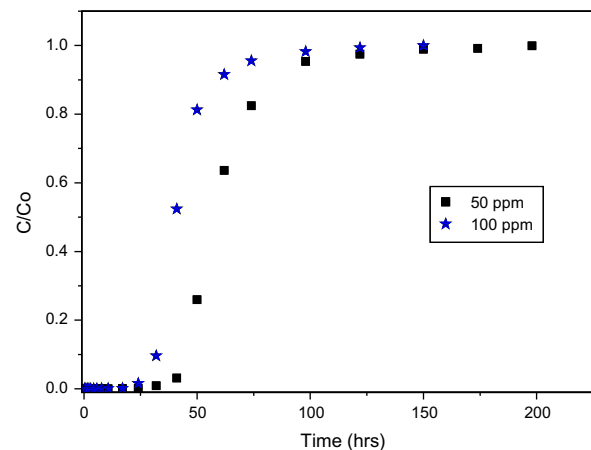


Fig. 8. The effect of inlet Cr(VI) concentration for the removal of Cr(VI) keeping the inlet flow rate and mass of adsorbent of 10 mL min⁻¹ and 75 g, respectively.

As the initial concentration of Cr(VI) is increased from 50 to 100 mg L⁻¹, the breakthrough time decreased from 24.78 to 13.875 h. The total time required for the adsorption is analogous to the stoichiometric capacity of the column and is found to be decreased from 110.7 to 57.4 h when the inlet concentration is increased from 50 to 100 mg L⁻¹ (Table 1). However, there is an increase in the fraction of the

Table 1

Different parameters for the removal of Cr(VI) from aqueous solution in a fixed-bed adsorption column for different operating conditions

S No	C_0 mg L^{-1}	Q mL min^{-1}	W g	t_t h	t_f h	t_b h	q_s mg g^{-1}	q_t mg	m_t mg	S %	EBRT s	R_a g L^{-1}	y
1	50	10	75	110.7	198	24.78	25.75	1858	3,321	55.92	15.21	5.04	0.6151
2	100	10	75	57.4	150	13.88	35.08	1,316	3,442	38.24	15.21	9.01	0.6836
3	50	5	75	135.8	222	35.09	16.62	1,246	2,036	61.17	30.41	7.13	0.5779
4	50	15	75	71.9	122	8.26	25.21	1,907	3,236	58.94	10.14	10.09	0.8034
5	50	10	25	75.7	198	9.25	34.57	868	2,270	38.23	5.07	4.50	0.6789
6	50	10	50	93.2	198	11.44	26.23	1,316	2,795	47.06	10.14	7.28	0.7383
7	50	10	100	147.7	246	50.24	26.61	2,659	4,429	60.02	20.28	3.32	0.4337
8	50	10	125	176.9	270	74.15	27.65	3,478	5,307	65.52	25.35	2.81	0.3563
9	50	10	150	204.8	294	98.23	28.42	4,282	6,145	69.68	30.41	2.55	0.3086
10	50	10	175	231.8	318	111.6	28.89	5,069	6,954	72.89	35.48	2.61	0.3374

unused bed length from 0.61 to 0.68. The total percentage removal of Cr(VI) decreases from 55.92 to 38.24%, while the adsorbent exhaustion rate increases from 5.04 to 9.01 g L^{-1} with an increase in the inlet Cr(VI) concentration from 50 to 100 mg L^{-1} (Table 1).

The bed saturation and the breakthrough time are obtained earlier with an increase in the initial concentration due to the relatively slower rate of mass transfer. The decrease in mass transfer rate is due to the reduced mass transfer coefficient and diffusion coefficient at low Cr(VI) concentration [17]. The decrease in the breakthrough time may be a result of faster saturation of ANB as the more molecules of Cr(VI) are available to saturate the active sites.

4.2. Effect of mass of adsorbent

The effect of the mass of the adsorbent on the breakthrough curve is studied for variable mass that is 25, 50, 75, 100, 125, 150 and 175 g, and is shown in Fig. 9. The other parameters such as the flow rate and initial concentration of Cr(VI) are maintained constant at 10 ml min^{-1} and 50 mg L^{-1} , respectively.

With an increase in the mass of the adsorbent from 25 to 175 g, the time acquired for breakthrough is increased from 9.25 to 111.66 h and the total time required corresponding to the stoichiometric capacity of the column increases from 75.7 to 231.8 h (Table 1). This may be due to the increase in the availability of the number of active sites for the removal of Cr(VI) [45]. The total percentage removal of the Cr(VI) increases from 38.23 to 72.89%, however, the fraction of the unused bed length and the adsorbent exhaustion rate decreases from 0.74 to 0.34 and from 7.284 to 2.612 g L^{-1} , respectively, with an increase in the mass

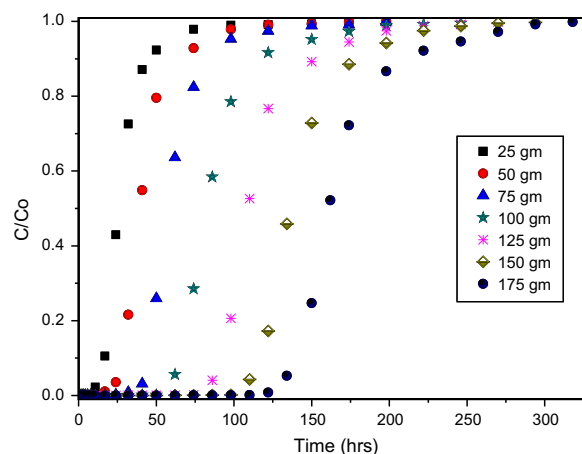


Fig. 9. The effect of mass of adsorbent for the removal of Cr(VI) keeping the inlet flow rate and concentration constant at 10 ml min^{-1} and 50 mg L^{-1} , respectively.

of the adsorbent from 25 to 175 g (Table 1). The adsorbent exhaustion rate decreases with an increase in mass of adsorbent which depicts the faster exhaustion of the adsorbent for a smaller amount.

4.3. Effect of flow rate

The effect of flow rate on the breakthrough curve is studied by varying the flow rate from 5 to 15 ml min^{-1} while keeping the mass of the adsorbent and initial concentration constant at 75 g and 50 mg L^{-1} , respectively (Fig. 10).

With an increase in the flow rate from 5 to 15 ml min^{-1} , there is a decrease in the breakthrough time from 35.09 to 8.26 h (Table 1). This decrease in

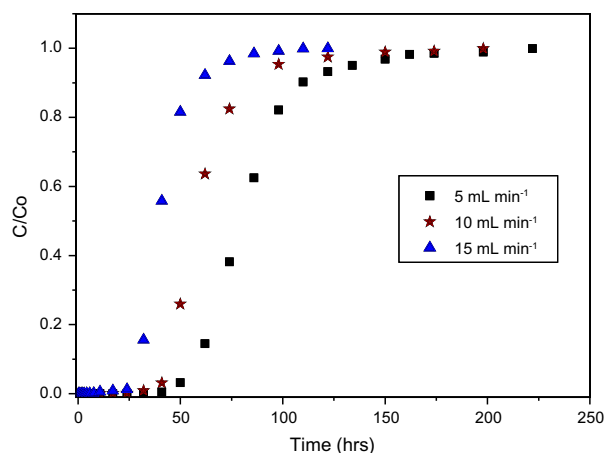


Fig. 10. The effect of flow rate for the removal of Cr(VI) keeping the mass of the adsorbent and concentration constant at 75 g and 50 mg L⁻¹, respectively.

the breakthrough time may be due to the availability of more amount of Cr(VI) for adsorption. Besides, there is a decrease in the total percentage removal from 61.17 to 55.92% when the flow rate is increased from 5 to 10 ml min⁻¹. With an increase in the flow rate, there is a decrease in residence time, which may lead to the steepness of the breakthrough curve and the reduction in the overall percentage removal of Cr(VI). The faster rate is restricting down the removal to attain equilibrium during the process. With an increase in the flow rate from 5 to 15 ml min⁻¹, the total time required corresponding to the stoichiometric capacity of the column decreases from 135.8 to 71.9 h and the fraction of the unused bed length increases from 57.79 to 80.33 (Table 1).

The saturation loading (q_s) for Cr(VI) from the above analysis is obtained as approximately 27.5 mg g⁻¹ which is found to be very close to the adsorption capacity value (26.95 mg g⁻¹) obtained from batch equilibrium study [22].

4.4. Effect of other metal ions

In today's era, with the industrialization, the composition of the effluents is changing drastically. There are multiple metal ions present in the effluents from various industries such as textile, paper and pulp and metal finishing. Hence, it is very important to study the performance of ANB for the removal of Cr(VI) from wastewater in the presence of other metal ions [Cu(II), Zn(II), etc.]. This study would indicate the feasibility for the use of ANB to treat more practical industrial effluents. The aqueous solution contains 50 mg L⁻¹ each of Cr(VI), Zn(II) and Cu(II). The flow

rate and mass of adsorbent for this experiment are maintained as 10 ml min⁻¹ and 75 g, respectively. The breakthrough curves for the simultaneous removal of Cr(VI), Cu(II) and Zn(II) are shown in Fig. 11. The breakthrough curve for Cr(VI) removal at the same operating conditions in the absence of other metal ions is also shown in Fig. 11 for the comparison purpose.

It is observed that the breakthrough time is attained in 9.25 h which is earlier than the time achieved, that is 24.78 h in the experiment performed for the pure Cr(VI) aqueous solution. This decrease in the breakthrough time is due to the simultaneous utilization of the adsorbent for the removal of Cr(VI), Cu(II) and Zn(II) present in the solution. The presence of Cu(II) and Zn(II) along with Cr(VI) on adsorption sites has been already established by the EDS image (Fig. 4) of the used adsorbent. The saturation loading for the Cr(VI) adsorption system is found out to be 20.64 mg g⁻¹ which is less than what is obtained for the pure Cr(VI) solution. In the multiple ions adsorption experiment, the saturation loadings for Cu(II) and Zn(II) removal are obtained as 16.29 and 17.02 mg g⁻¹, respectively. These obtained values are significantly high as compared to the reported adsorption capacities of low-cost adsorbents.

On calculating the various parameters for the multiple metal ion, the average saturation loading for either of the metal ions (Cr(VI), Cu(II) and Zn(II)) is coming to be 26.485 mg g⁻¹ while the saturation loading for the multiple metal ions feed is coming to be 53.95 mg g⁻¹ which is approximately double to that of the pure feed. Further, the presence of multiple metal ions decreases the percentage removal of individual metal ions by approximately 11.81% in comparison with their pure runs. However, the simultaneous

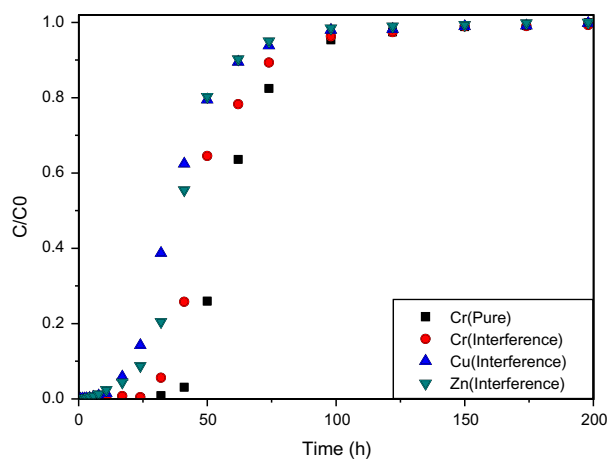


Fig. 11. The effect of the presence and absence of multiple metal ions (Cu & Zn) on the removal of Cr(VI).

Table 2
Different parameters for the Yoon–Nelson and Yan models

Inlet Conc. C_0 (mg L^{-1})	Flow rate (mL min^{-1})	Mass of adsorbent (g)	Yoon–Nelson model				Yan model			
			$K_{YN,i}$ (h^{-1})	τ_i (h)	R^2	χ^2	$q_{0,i}$	a_i	R^2	χ^2
50	10	75	7.8421	0.9801	0.997	0.00057	0.00039	7.2297	0.999	0.00023
100	10	75	11.5468	0.6902	0.997	0.00068	0.00055	7.5469	0.998	0.00031
50	5	75	5.2716	1.3453	0.998	0.00035	0.00027	6.8365	0.999	0.00008
50	15	75	10.7027	0.6764	0.998	0.0005	0.0004	6.8545	0.999	0.00015
50	10	25	11.0256	0.4457	0.996	0.00084	0.00052	4.4189	0.999	0.00012
50	10	50	9.4744	0.6728	0.998	0.00043	0.0004	5.7928	0.999	0.00015
50	10	100	6.1128	1.3962	0.997	0.00053	0.00042	7.9832	0.999	0.00024
50	10	125	6.3935	1.8358	0.997	0.00062	0.00044	10.9404	0.998	0.00043
50	10	150	5.1619	2.3046	0.997	0.00054	0.00046	11.3097	0.998	0.00031
50	10	175	4.8684	2.7135	0.996	0.00067	0.00046	12.4273	0.997	0.00046

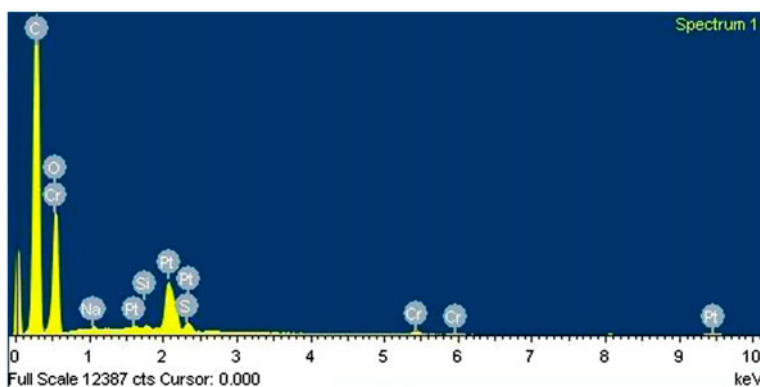


Fig. 12. EDX analysis of the regenerated adsorbent used on Cr(VI).

removal of all the three metals is considerably high. This indicates that the developed adsorbent, ANB, is more suitable to treat the wastewater containing multiple metal ions, that is more efficient and economical to treat the industrial effluent.

4.5. Evaluation of the kinetic parameters from column data modelling

The experimental data of the breakthrough curves are fitted with the Yoon–Nelson and Yan models using the non-linear regression method of Origin 6.0 software. The values of the different parameters for the Yoon–Nelson and Yan models are being tabulated in Table 2.

The values obtained from the Yoon–Nelson model infer that the $K_{YN,i}$ increases from 7.84207 to 11.5468 h^{-1}

and 5.2715 to 10.7027 h^{-1} with an increase in the inlet concentration (50 to 100 mg L^{-1}) and the flow rate (5 min^{-1} to 15 ml min^{-1}), respectively. It decreases from 11.0256 to 4.8684 h^{-1} when the mass of the adsorbent increases from 25 to 175 g. The value of the τ_i decreases from 0.9801 to 0.6902 h and 1.3453 to 0.6764 h with an increase in the inlet concentration (50 to 100 mg L^{-1}) and the flow rate (5 to 15 ml min^{-1}), respectively. The value τ_i increases from 0.4457 to 2.7035 h when the mass of the adsorbent increases from 25 to 175 g.

Although the R^2 value are better for the Yan model, but the trends for the model parameters are very irregular with the variation of various parameter values. Also, the R^2 value for Yoon–Nelson model are near about to Yan model. Hence, in the present study, the applicability of Yoon–Nelson model for the scaling up of the process is more justifiable.

5. Regeneration

The used adsorbent, containing Cr(VI), is not safe to be disposed off as a solid waste due to the various environmental restrictions. This leads to a fact of regenerating the adsorbent for its reuse. In the present study, the adsorbent is tried to be regenerated thermodynamically. The used adsorbent is kept for washing in distilled water at 90°C for 2 h on a rotary shaker. It is found that 40% of the Cr(VI) is recovered and the ANB is again available for the use. The EDX analysis showing the decrease in the Cr(VI) content on the adsorbent surface is being provided in Fig. 12.

6. Conclusions

In the present work, neem bark is activated and is utilized as ANB for the removal of Cr(VI) in a continuous fixed-bed column. The effect of the mass of adsorbent, metal inlet concentration and flow rate is evaluated and found to have a strong influence on the breakthrough curves. With an increase in the mass of adsorbent from 25 to 175 g, inlet concentration from 50 to 100 mg L⁻¹ and flow rate from 5 to 15 mg L⁻¹, the breakthrough time increases from 9.25 to 111.66 h, decreases from 24.78 to 13.875 h and 35.086 to 8.262 h, respectively. The average saturation loading capacity of the column is found to be approximately 27.5 mg g⁻¹ which is in alignment with the adsorption capacity 26.9 mg g⁻¹ obtained in the batch equilibrium study. The developed adsorbent has shown good applicability for treating the wastewater containing multiple metal ions. It is found that the saturation loading of the adsorbent increases to 53.95 for multiple metal ions in comparison with an average of 26.485 mg g⁻¹ for an individual metal ion. The experimental data are found to be well described by the Yoon–Nelson kinetic model.

Acknowledgments

The authors would like to thank the University Grants Commission (UGC), New Delhi, and the Department of Science & Technology (DST), New Delhi, for their financial assistance.

References

- [1] S. Mohan, G. Sreelakshmi, Fixed bed column study for heavy metal removal using phosphate treated rice husk, *J. Hazard. Mater.* 153 (2008) 75–82.
- [2] B.V. Babu, S. Gupta, Adsorption of Cr(VI) using activated neem leaves: Kinetic studies, *Adsorption* 14 (2008) 85–92.
- [3] T. Shi, Z. Wang, Y. Liu, S. Jia, D. Changming, Removal of hexavalent chromium from aqueous solutions by D301, D314 and D354 anion-exchange resins, *J. Hazard. Mater.* 161 (2009) 900–906.
- [4] M. Gheju, I. Balcu, Removal of chromium from Cr(VI) polluted wastewaters by reduction with scrap iron and subsequent precipitation of resulted cations, *J. Hazard. Mater.* 196 (2011) 131–138.
- [5] C. Bertagnolli, M.G.C. da Silva, E. Guibal, Chromium biosorption using the residue of alginate extraction from *Sargassum filipendula*, *Chem. Eng. J.* 237 (2014) 362–371.
- [6] S. Gupta, B.V. Babu, Experimental, kinetic, equilibrium and regeneration studies for adsorption of Cr(VI) from aqueous solutions using low cost adsorbent (activated flyash), *Desalin. Water Treat.* 20 (2010) 168–178.
- [7] A.P. Padilla, E.L. Tavani, Treatment of an industrial effluent by reverse osmosis, *Desalination* 126 (1999) 219–226.
- [8] S. Gupta, B.V. Babu, Removal of toxic metal Cr(VI) from aqueous solutions using sawdust as adsorbent: Equilibrium, kinetics and regeneration studies, *Chem. Eng. J.* 150 (2009) 352–365.
- [9] G. Gangadhar, U. Maheshwari, S. Gupta, Application of nanomaterials for the removal of pollutants from effluent streams, *Nanosci. Nanotech. -Asia* 2 (2012) 140–150.
- [10] U. Maheshwari, A review on adsorption process for the removal of dyes from textile industry effluent, in: *AIChE (Ed.), 2013 AIChE Annual Meeting*, San Francisco, CA, 2013, pp. 276.
- [11] F. Fu, Q. Wang, Removal of heavy metal ions from wastewaters: A review, *J. Environ. Manage.* 92 (2011) 407–418.
- [12] M. Ahmaruzzaman, Industrial wastes as low-cost potential adsorbents for the treatment of wastewater laden with heavy metals, *Adv. Colloid Interface Sci.* 166 (2011) 36–59.
- [13] K.L. Wasewar, Adsorption of metals onto tea factory waste: A review, *Int. J. Res. Rev. Appl. Sci.* 3 (2010) 303–322.
- [14] D. Mohan, C.U. Pittman Jr., Activated carbons and low cost adsorbents for remediation of tri- and hexavalent chromium from water, *J. Hazard. Mater.* 137 (2006) 762–811.
- [15] S. Sugashini, K.M.M.S. Begum, Performance of ozone treated rice husk carbon (OTRHC) for continuous adsorption of Cr(VI) ions from synthetic effluent, *J. Environ. Chem. Eng.* 1 (2013) 79–85.
- [16] S. Gupta, B.V. Babu, Experimental investigations and theoretical modeling aspects in column studies for removal of Cr(VI) from aqueous solutions using activated tamarind seeds, *J. Water Resource Prot.* 2 (2010) 706–716.
- [17] S. Gupta, B.V. Babu, Modeling, simulation, and experimental validation for continuous Cr(VI) removal from aqueous solutions using sawdust as an adsorbent, *Bioresour. Technol.* 100 (2009) 5633–5640.
- [18] A.B. Pérez Marín, M.I. Aguilar, V.F. Meseguer, J.F. Ortuño, J. Sáez, Biosorption of chromium (III) by orange (*Citrus cinensis*) waste: Batch and continuous studies, *Chem. Eng. J.* 155 (2009) 199–206.
- [19] R. Rao, F. Rehman, Adsorption of heavy metal ions on pomegranate (*Punica Granatum*) peel: Removal and recovery of Cr(VI) ions from a multi-metal ion system, *Adsorpt. Sci. Technol.* 28 (2010) 195–211.

- [20] R.A.K. Rao, F. Rehman, Adsorption studies on fruits of Gular (*Ficus glomerata*): Removal of Cr(VI) from synthetic wastewater, *J. Hazard. Mater.* 181 (2010) 405–412.
- [21] R. Ali Khan Rao, F. Rehman, M. Kashifuddin, Removal of Cr(VI) from electroplating wastewater using fruit peel of Leechi (*Litchi Chinensis*), *Desalin. Water Treat.* 49 (2012) 136–146.
- [22] U. Maheshwari, S. Gupta, Kinetic and equilibrium studies of Cr (VI) removal from aqueous solutions using activated neem bark, *Res. J. Chem. Environ.* 15 (2011) 939–943.
- [23] K. Selvaraj, S. Manonmani, S. Pattabhi, Removal of hexavalent chromium using distillery sludge, *Bioresour. Technol.* 89 (2003) 207–211.
- [24] S.M. Contreras-Ramos, D. Alvarez-Bernal, N. Trujillo-Tapia, L. Dendooven, Composting of tannery effluent with cow manure and wheat straw, *Bioresour. Technol.* 94 (2004) 223–228.
- [25] R. Kumar, N.R. Bishnoi, Garima, K. Bishnoi, Biosorption of chromium(VI) from aqueous solution and electroplating wastewater using fungal biomass, *Chem. Eng. J.* 135 (2008) 202–208.
- [26] E. Malkoc, Y. Nuhoglu, Potential of tea factory waste for chromium(VI) removal from aqueous solutions: Thermodynamic and kinetic studies, *Sep. Purif. Technol.* 54 (2007) 291–298.
- [27] Z. Aksu, F. Gönen, Biosorption of phenol by immobilized activated sludge in a continuous packed bed: Prediction of breakthrough curves, *Process Biochem.* 39 (2004) 599–613.
- [28] K.H. Chu, Improved fixed bed models for metal biosorption, *Chem. Eng. J.* 97 (2004) 233–239.
- [29] A. Keshtkar, F. Kafshgari, M. Mousavian, Binary biosorption of uranium(VI) and nickel(II) from aqueous solution by Ca-pretreated *Cystoseira indica* in a fixed-bed column, *J. Radioanal. Nucl. Chem.* 292 (2012) 501–512.
- [30] B. Salamatina, A.H. Kamaruddin, A.Z. Abdullah, Modeling of the continuous copper and zinc removal by sorption onto sodium hydroxide-modified oil palm frond in a fixed-bed column, *Chem. Eng. J.* 145 (2008) 259–266.
- [31] Y.H. Yoon, J.H. Nelson, Application of gas adsorption kinetics I. A theoretical model for respirator cartridge service life, *Am. Ind. Hyg. Assoc. J.* 45 (1984) 509–516.
- [32] M. Calero, F. Hernáinz, G. Blázquez, G. Tenorio, M.A. Martín-Lara, Study of Cr(III) biosorption in a fixed-bed column, *J. Hazard. Mater.* 171 (2009) 886–893.
- [33] G. Yan, T. Viraraghavan, M. Chen, A new model for heavy metal removal in a biosorption column, *Adsorpt. Sci. Technol.* 19 (2001) 25–43.
- [34] S. Gupta, B.V. Babu, Utilization of waste product (tamarind seeds) for the removal of Cr(VI) from aqueous solutions: Equilibrium, kinetics, and regeneration studies, *J. Environ. Manage.* 90 (2009) 3013–3022.
- [35] C. Namasivayam, M.V. Sureshkumar, Removal of chromium(VI) from water and wastewater using surfactant modified coconut coir pith as a biosorbent, *Bioresour. Technol.* 99 (2008) 2218–2225.
- [36] J. Guo, Y. Li, R. Dai, Y. Lan, Rapid reduction of Cr(VI) coupling with efficient removal of total chromium in the coexistence of Zn(0) and silica gel, *J. Hazard. Mater.* 243 (2012) 265–271.
- [37] M.A. Hossain, M. Kumita, S. Mori, Sem characterization of the mass transfer of Cr(Vi) during the adsorption on used black tea leaves, *Afr. J. Pure Appl. Chem.* 4 (2010) 135–141.
- [38] A. Kumar, N.N. Rao, S.N. Kaul, Alkali-treated straw and insoluble straw xanthate as low cost adsorbents for heavy metal removal—preparation, characterization and application, *Bioresour. Technol.* 71 (2000) 133–142.
- [39] M. Bakiler, I.V. Maslov, S. Akyüz, Theoretical study of the vibrational spectra of 2-chloropyridine metal complexes II. Calculation and analysis of the IR spectra of Cd- and Ni-2-Chloropyridine complexes, *J. Mol. Struct.* 476 (1999) 21–26.
- [40] K. Kaya, E. Pehlivan, C. Schmidt, M. Bahadir, Use of modified wheat bran for the removal of chromium(VI) from aqueous solutions, *Food Chem.* 158 (2014) 112–117.
- [41] T. Depci, A.R. Kul, Y. Önal, Competitive adsorption of lead and zinc from aqueous solution on activated carbon prepared from Van apple pulp: Study in single- and multi-solute systems, *Chem. Eng. J.* 200–202 (2012) 224–236.
- [42] M.R. Taha, A.H. Ibrahim, Characterization of nano zero-valent iron (nZVI) and its application in Sono-Fenton process to remove COD in palm oil mill effluent, *J. Environ. Chem. Eng.* 2 (2014) 1–8.
- [43] S. Maiti, J. Jayaramudu, K. Das, S.M. Reddy, R. Sadiku, S.S. Ray, D. Liu, Preparation and characterization of nano-cellulose with new shape from different precursor, *Carbohydr. Polym.* 98 (2013) 562–567.
- [44] U. Maheshwari, S. Gupta, Removal of Cr(Vi) from wastewater using a natural nanoporous adsorbent: Experimental, kinetic and optimization studies, *Adsorpt. Sci. Technol.* 33(2015) 71–88.
- [45] L. Deng, Z. Shi, B. Li, L. Yang, L. Luo, X. Yang, Adsorption of Cr(VI) and phosphate on Mg–Al hydrotalcite supported kaolin clay prepared by ultrasound-assisted coprecipitation method using batch and fixed-bed systems, *Ind. Eng. Chem. Res.* 53 (2014) 7746–7757.